




PERFORMANCE ANALYSIS OF RIS-EQUIPPED UAV COMMUNICATION NETWORK UNDER HARDWARE IMPAIRMENTS

Nhat-Tien NGUYEN¹ , Hong-Nhu NGUYEN¹ , Minh-Vu BUI^{2,*} 

¹Faculty of Engineering and Technology, Saigon University, 273 An Duong Vuong street, Ward 2, District 5, Ho Chi Minh City, Vietnam

²Faculty of Engineering and Technology, Nguyen Tat Thanh University, Ho Chi Minh City, Vietnam

tien.nn@sgu.edu.vn, nhu.nh@sgu.edu.vn, bvminh@ntt.edu.vn

*Corresponding author: Minh-Vu Bui; bvminh@ntt.edu.vn

DOI: 10.15598/aece.v23i3.250211

Article history: Received Feb 27, 2025; Revised May 04, 2025; Accepted May 21, 2025; Published Sep 30, 2025.
This is an open access article under the BY-CC license.

Abstract. *Reconfigurable Intelligent Surfaces (RIS) are recognized as a promising technology that boosts spectral efficiency, elevates data speeds, and minimizes latency. This study explores the performance of UAV communication networks that are equipped with RIS to serve edge users, particularly considering the effects of hardware impairments within Rician-fading channels. By using the moment method to simplify the analysis, we derive the probability density function (PDF) and cumulative distribution function (CDF) for the system. Furthermore, we derive the asymptotic outage probability (OP) to gain insights into system performance at high signal-to-noise ratio (SNR). Numerical results validate the analytical derivations and illustrate the influence of the main parameter into the system.*

IoT system, the development of energy-efficient, high-bandwidth wireless technology is becoming essential [1–4]. Reconfigurable intelligent surfaces (RIS) represent a transformative technology in wireless communication, capable of modifying the wireless environment to enhance spectrum and energy efficiency. It is regarded as an outstanding opportunity and a legitimate green resolution initiative in the forthcoming wireless communication [6–8]. In particular, RIS consists of surfaces composed of electromagnetic materials regulated by integrated electronic devices with distinctive wireless communication functionalities. The intelligent radio environment is a wireless network that converts the wireless network landscape into a reconfigurable intelligent space, managed by telecommunications operators, and facilitates effective information transmission and processing [9–11].

Keywords

Outage probability, UAV, RIS, hardware impairment

1. Introduction

The Internet of Things (IoT) technology is garnering significant interest due to its vast potential to interconnect billions of devices across many applications. Motivated by economic and environmental considerations, as well as the magnitude of the forthcoming

The UAV-assisted communication system has attracted widespread attention in recent years due to its on-demand deployment, high flexibility, and low cost [12,13]. One of the most significant advantages of building a UAV-assisted wireless communication network is that it is easy to build a line-of-sight (LoS) channel between the UAV and the ground user, for ease of enhancing the system performance [14,15]. The authors in [16] have examined the civil uses of UAV networks from a communication standpoint, including their features. They furthermore presented experimental findings from other studies. A study report by the authors in [17] detailed many challenges faced in UAV communication networks to provide robust and

Tab. 1: Comparison between the novelty of our work and previous papers.

Ref./Prop.	UAV-RIS	Hardware impairment	OP Expression	Diversity order	EC Expression
[32]	✓	X	✓	✓	✓
[33]	✓	X	✓	✓	✓
[34]	✓	X	✓	X	X
[35]	✓	✓	✓	✓	X
Our study	✓	✓	✓	✓	✓

dependable wireless transmission. [18] conducted an extensive study and emphasized the possibilities for the provision of low-altitude UAV-based IoT services via aerial platforms. The cybersecurity of UAVs was examined in [19], addressing both real and simulated threats. Additionally, [20] examined the most prominent routing protocols for UAVs and evaluated the performance of the leading current routing protocols. The trade-off between reliability and security in UAV communications employing energy harvesting relays was comprehensively investigated in [21]. The study highlighted the impact of energy harvesting constraints on both the reliability of data transmission and the confidentiality of sensitive information, offering insights into optimizing system design under such dual objectives.

On another hand, the RIS-equipped UAV communications is a promising technology that improves service delivery to users at the edge or in locations where direct transmission is challenging [22–29]. In particular, [22] investigated the performance of the RIS-equipped UAV-based emergency wireless communication system by getting the new channel statistics for the probability density function (PDF) and cumulative distribution function (CDF), and deriving the closed-form expression for the achievable rate, bit error rate (BER), and outage probability (OP). In the RIS-equipped UAV system equipped with energy harvesting capabilities, the authors in [23] have introduced the mathematical expressions to derive the OP, effective throughput, and average bit error rate of the system. In [25], the authors developed a RIS coupled to a UAV inside a massive multiple-input multiple-output (MIMO) network and articulated a method for determining the optimal power control coefficients at the base station and phase shifts of the RIS to maximize overall throughput. In [26], the secrecy performance of RIS-assisted satellite communication networks under Shadowed-Rician fading channels was investigated. The authors derived closed-form expressions for the secrecy outage probability (SOP) and a lower bound on the secrecy capacity, thereby providing analytical insights into the influence of RIS configuration parameters and satellite channel characteristics on secure communications. Extending this line of inquiry, [27] analyzed RIS-assisted satellite-UAV cooperative communication networks, explicitly considering the impact of RIS phase alignment errors.

In addition, [28] proposed a novel partial multiplexing power-frequency multiple access (PFMA) scheme for simultaneously transmitting and reflecting RIS (STAR-RIS)-assisted networks. This strategy aimed to eliminate the need for successive interference cancellation while enhancing spectral and energy efficiency. The authors derived closed-form expressions for the outage probability and ergodic capacity under Nakagami-m fading, and formulated a joint power and bandwidth allocation optimization problem to maximize overall system throughput. By leveraging active reconfigurable repeaters, the authors in [29] addressed the simultaneous requirements of reliability, security, and covertness, paving the way for enhanced performance in both terrestrial and aerial communication scenarios. In practical communication systems, the transmitter and receiver hardware of wireless nodes are often influenced by non-ideal properties, such as I/Q imbalance, amplifier amplitude nonlinearity, and phase noise (Residual Hardware Impairment, RHI) [30, 31]. To the best of our knowledge, there are no work concerns on the performance of RIS-equipped UAV communication in the context of hardware limitations. Table 1 show the comparison between the novelty of our work and previous papers. Thus, the primary contribution may be summarized as follows:

- We proposed the RIS-equipped UAV communication network under the presence of imperfect with the channels follows Rician fading channels. Furthermore, a source transmits the signal to the device with the help of the RIS-equipped UAV by setting the optimal phase shift.
- By applying the moment method, we presented the new channel statistics for the PDF and CDF. Next, the closed-form and approximated expressions for OP and average ergodic capacity (EC) are derived. The asymptotic OP is also expressed to get insight on the proposed system.
- We presented the numerical results and discussion to verify our analysis and show the impact of the main parameters on the system.

The subsequent sections of this work are summarized as follows: Section 2. describes the system model of the suggested schemes. The derivation for

the performance of the system is conducted in Section 3. Section 4. presents simulation and theoretical findings, while Section 5. concludes the paper.

Notations: $E\{\cdot\}$ is the expectation, $I_0(z)$ is the zero-order modified Bessel function of the first kind [51, Eq. 8.445], $K_v(x)$ is the modified Bessel function of the second kind [51, Eq. 8.446], $\Gamma(x)$ denotes the Gamma function [51, Eq. 8.310], $\gamma(\cdot, \cdot)$, $\Gamma(\cdot, \cdot)$ are the upper and lower incomplete Gamma functions [51, Eq. 8.350].

2. System Model

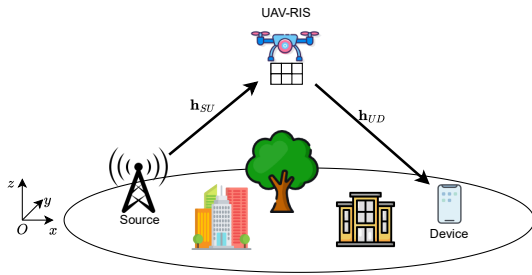


Fig. 1: A proposed UAV-RIS system model.

In this paper, we considered a UAV-aided RIS communication network that includes a source (S), UAV-RIS (U) composed of N reflecting meta-surfaces, and a device (D) as in Figure 1, where S , and D are equipped with a single antenna. Usually, metropolitan structures and mountains may obstruct or hinder the connection between the source and terminal devices. In these cases, UAV-RIS is needed to implement aided communication and improve the signal quality. Moreover, we assume that all channels are independent and identically distributed (i.i.d.) and that the RIS controller can acquire comprehensive channel state information (CSI) [36]. Regarding the UAV network, we consider the three-dimensional Cartesian coordinate (x, y, z) illustrated in Figure 1. Furthermore, the UAV-RIS is located at $(r_U \cos(\varphi_U), r_U \sin(\varphi_U), z_U)$ as [42], where we consider the fixed-wing UAV-RIS to have a circular trajectory with a radius r_U , altitude z_U and the angle φ_U . In addition, the S and D are located at $(x_S, y_S, 0)$, and $(x_D, y_D, 0)$, respectively. Based on these results, we are able to determine the Euclidean distance from S to U and U to D as follows:

$$d_{SU} = \sqrt{(r_U \cos(\varphi_U) - x_S)^2 + (r_U \sin(\varphi_U) - y_S)^2 + (z_U)^2}, \quad (1a)$$

$$d_{UD} = \sqrt{(x_D - r_U \cos(\varphi_U))^2 + (y_D - r_U \sin(\varphi_U))^2 + (z_U)^2}, \quad (1b)$$

Due to the UAVs' high altitude, the UAV-ground channels often have a strong LoS connection with some multi-path components because of the ground's reflection/scattering, vegetation, etc. [37]. According to [38], the channel of UAV-ground can be modeled by Rician fading. Moreover, the Rician factor and path-loss coefficient are given respectively as [39]

$$K_j = \alpha_1 e^{\alpha_2 \kappa_j}, \quad \tau_j = \alpha_3 P_{LoS} + \alpha_4, \quad (2)$$

where $j \in \{SU, UD\}$, $P_{LoS} = (1 + \alpha_5 e^{-\alpha_6 \kappa_j + \alpha_5})^{-1}$ denotes the LoS probability, $\kappa_j = \arcsin\left(\frac{h}{d_j}\right)$ is the elevation angle and $\alpha_1, \alpha_2, \alpha_3, \alpha_4, \alpha_5, \alpha_6$ are the environment and frequency dependent constants. Next, under the hardware impairment, the actual received signal at D is given as

$$y_D = \sum_{n=1}^N \frac{h_{SU_n} h_{UD_n} e^{j\varphi_n}}{\sqrt{d_{SU}^{\tau_{SU}} d_{UD}^{\tau_{UD}}}} (x_S + \eta_t) + \eta_r + n_D, \quad (3)$$

where x_S is the transmit signal and $E\{|x_S|^2\} = P_S$ with P_S is the transmit power, $n_D \sim CN(0, N_0)$ denotes the additive white Gaussian noise (AWGN), φ_n denotes the phase shift of n -th reflecting element of UAV-RIS, $h_{SU_n} = g_{SU_n} e^{-j\psi_n}$, and $h_{UD_n} = g_{UD_n} e^{-j\theta_n}$ are the channel coefficients from S to n -th reflecting element of UAV-RIS and from n -th reflecting element of UAV-RIS to D , respectively, ψ_n and θ_n are the phases of the channel, g_{SU_n} , and g_{UD_n} are the magnitudes of the channel coefficients, $\eta_t \sim CN(0, \kappa_t^2 P_S)$ denotes the distortion noise from source, $\eta_r \sim CN(0, \frac{\kappa_r^2 Z^2 P_S}{d_{SU}^{\tau_{SU}} d_{UD}^{\tau_{UD}}})$ denotes the distortion noise from device, κ_t, κ_r are measured as error vector magnitudes (EVMS), and $Z = \left| \sum_{n=1}^N h_{SU_n} h_{UD_n} \right|$. Next, by setting $\varphi_n = \psi_n + \theta_n$ [40, 41], the maximized instantaneous signal-to-distortion-plus-noise ratio (SDNR) at D is given by

$$\begin{aligned} \gamma_D &= \frac{P_S Z^2}{P_S \kappa_t^2 Z^2 + P_S \kappa_r^2 Z^2 + d_{SU}^{\tau_{SU}} d_{UD}^{\tau_{UD}} N_0} \\ &= \frac{\rho Z^2}{(\kappa_t^2 + \kappa_r^2) \rho Z^2 + d_{SU}^{\tau_{SU}} d_{UD}^{\tau_{UD}}}, \end{aligned} \quad (4)$$

where $\rho = \frac{P_S}{N_0}$ is the average signal-to-noise ratio (SNR).

3. Performance Analysis of UAV-RIS network

3.1. Channel modeled

To calculate the system performance metrics further, we consider all the channel coefficients to follow Rician

fading. Thus, the PDF of g_j is given as [42–44]

$$f_{g_j}(x) = \frac{2(1+K_j)e^{-K_jx}}{\Omega_j e^{\frac{(1+K_j)}{\Omega_j}x^2}} I_0 \left(2\sqrt{\frac{K_j(1+K_j)}{\Omega_j}} x \right), \quad (5)$$

where Ω_j denotes the average power, we can express as

$$f_{g_j}(x) = \sum_{k=0}^{\infty} \frac{2(K_j)^k e^{-K_j}}{(k!)^2 e^{\frac{(1+K_j)}{\Omega_j}x^2}} \left(\frac{(1+K_j)}{\Omega_j} \right)^{k+1} x^{2k+1}. \quad (6)$$

Furthermore, the PDF of $Z_n \triangleq g_{SU_n} g_{UD_n}$ can be calculated as

$$f_{Z_n}(x) = \int_0^{\infty} \frac{1}{y} f_{g_{SU_n}}(y) f_{g_{UD_n}}\left(\frac{x}{y}\right) dy. \quad (7)$$

With the help of (5), we can formulate as

$$\begin{aligned} f_{Z_n}(x) &= \sum_{k_1=0}^{\infty} \sum_{k_2=0}^{\infty} \frac{4(K_{SU})^{k_1} (K_{UD})^{k_2} x^{2k_2+1}}{(k_1!)^2 (k_2!)^2 e^{K_{SU}+K_{UD}}} \\ &\times \left(\frac{(1+K_{SU})}{\Omega_{SU}} \right)^{k_1+1} \left(\frac{(1+K_{UD})}{\Omega_{UD}} \right)^{k_2+1} \\ &\times \int_0^{\infty} y^{2k_1-2k_2-1} e^{-\frac{(1+K_{SU})}{\Omega_{SU}}y^2 - \frac{(1+K_{UD})}{\Omega_{UD}}\left(\frac{x}{y}\right)^2} dy. \end{aligned} \quad (8)$$

Based on [51, Eq. 3.471.9] and after some algebraic manipulations, $f_Z(x)$ can be obtained as

$$\begin{aligned} f_{Z_n}(x) &= \sum_{k_1=0}^{\infty} \sum_{k_2=0}^{\infty} \frac{4(K_{SU})^{k_1} (K_{UD})^{k_2}}{(k_1!)^2 (k_2!)^2 e^{K_{SU}+K_{UD}}} \\ &\times \left(\frac{(1+K_{SU})(1+K_{UD})}{\Omega_{SU}\Omega_{UD}} \right)^{\frac{k_1+k_2+2}{2}} \\ &\times x^{k_1+k_2+1} K_{k_1-k_2} \left(2\sqrt{\frac{(1+K_{UD})(1+K_{SU})}{\Omega_{UD}\Omega_{SU}}} x \right). \end{aligned} \quad (9)$$

Based on the PDF of Z_n , we can derive the l -th moment of Z_n , which is obtained as follows:

$$\mu_{Z_n}(l) = E[Z_n^l] = \int_0^{\infty} x^l f_{Z_n}(x) dx. \quad (10)$$

From (9) and after some mathematical manipulations, we can be obtained by

$$\begin{aligned} \mu_{Z_n}(l) &= \sum_{k_1=0}^{\infty} \sum_{k_2=0}^{\infty} \frac{(K_{SU})^{k_1} (K_{UD})^{k_2}}{(k_1!)^2 (k_2!)^2 e^{K_{SU}+K_{UD}}} \\ &\times \left(\sqrt{\frac{\Omega_{SU}\Omega_{UD}}{(1+K_{SU})(1+K_{UD})}} \right)^l \\ &\times \Gamma\left(\frac{l}{2} + k_1 + 1\right) \Gamma\left(\frac{l}{2} + k_2 + 1\right), \end{aligned} \quad (11)$$

Based on the l -th moment of Z_n , we can approximate Z_n to a gamma distribution, and Z to a sum gamma distribution. Furthermore, the PDF and CDF of Z can be defined as

$$f_Z(x) = \frac{x^{\alpha_Z-1} (\beta_Z)^{\alpha_Z}}{\Gamma(\alpha_Z)} e^{-\beta_Z x}, \quad (12)$$

$$F_Z(x) = \frac{\gamma(\alpha_Z, \beta_Z x)}{\Gamma(\alpha_Z)}, \quad (13)$$

where

$$\alpha_Z = \frac{N(E[Z_n])^2}{\text{Var}[Z_n]} = \frac{N[\mu_{Z_n}(1)]^2}{\mu_{Z_n}(2) - [\mu_{Z_n}(1)]^2}, \quad (14)$$

$$\beta_Z = \frac{E[Z_n]}{\text{Var}[Z_n]} = \frac{\mu_{Z_n}(1)}{\mu_{Z_n}(2) - [\mu_{Z_n}(1)]^2}. \quad (15)$$

Moreover, after some variable substitutions and manipulations with $F_{Z^2}(x) = F_Z(\sqrt{x})$ and $f_{Z^2}(x) = 1/[2\sqrt{x}]f_Z(\sqrt{x})$, the PDF and CDF of Z^2 are respectively defined by

$$f_{Z^2}(x) = \frac{(\beta_Z)^{\alpha_Z}}{2\Gamma(\alpha_Z)} x^{\frac{\alpha_Z-2}{2}} e^{-\beta_Z \sqrt{x}}, \quad (16)$$

$$F_{Z^2}(x) = \frac{\gamma(\alpha_Z, \beta_Z \sqrt{x})}{\Gamma(\alpha_Z)}. \quad (17)$$

3.2. Outage probability Analysis

The OP is defined as the instantaneous SDNR below the threshold. Thus, the OP at D can be given by

$$P_{out} = \Pr(\gamma_D < \gamma_{th}), \quad (18)$$

where $\gamma_{th} = 2^{R_{th}} - 1$ and R_{th} are the target rates. From (4), the OP can be rewritten as

$$P_{out} = \Pr\left(Z^2 < \frac{\gamma_{th} d_{SU}^{\tau_{SU}} d_{UD}^{\tau_{UD}}}{\rho[1 - \gamma_{th}(\kappa_t^2 + \kappa_r^2)]}\right). \quad (19)$$

With help (17), the closed-form expression of OP at D is obtained as

$$P_{out} = \begin{cases} \frac{\gamma(\alpha_Z, \beta_Z \sqrt{\frac{\gamma_{th} d_{SU}^{\tau_{SU}} d_{UD}^{\tau_{UD}}}{\rho[1 - \gamma_{th}(\kappa_t^2 + \kappa_r^2)]}})}{\Gamma(\alpha_Z)} & \gamma_{th} < \frac{1}{(\kappa_t^2 + \kappa_r^2)} \\ 1 & \gamma_{th} > \frac{1}{(\kappa_t^2 + \kappa_r^2)} \end{cases} \quad (20)$$

To get the insight into the proposed system, the asymptotic OP at D in high SNR (i.e. $\rho \rightarrow \infty$) is analyzed. By applying the series representation of the incomplete Gamma function in [51, Eq. 8.354.1], we get

$$\gamma(\alpha, \beta x) \stackrel{x \rightarrow \infty}{\approx} \frac{(\beta x)^\alpha}{\alpha}. \quad (21)$$

Putting (21) into (20), the asymptotic OP at D is obtained as

$$P_{out}^{\infty} \approx \frac{(\beta_Z)^{\alpha_Z}}{\Gamma(N\alpha_Z + 1)} \left(\frac{\gamma_{th} d_{SU}^{\tau_{SU}} d_{UD}^{\tau_{UD}}}{\rho[1 - \gamma_{th}(\kappa_t^2 + \kappa_r^2)]} \right)^{\frac{\alpha_Z}{2}}. \quad (22)$$

From (21), the diversity order of the proposed system is $\frac{\alpha_Z}{2}$ in high SNR $\rho \rightarrow \infty$.

3.3. The average ergodic capacity

The average EC of the system can be calculated by

$$\bar{C}_D = E[\log_2(1 + \gamma_D)] = \frac{1}{\ln 2} \int_0^{\frac{1}{(\kappa_t^2 + \kappa_r^2)}} \frac{1 - F_{\gamma_D}(x)}{1 + x} dx. \quad (23)$$

Where $F_{\gamma_D}(x)$ is expressed as

$$F_{\gamma_D}(x) = \begin{cases} 1 - \frac{\Gamma\left(\alpha_Z, \beta_Z \sqrt{\frac{x d_{SU}^{\tau_{SU}} d_{UD}^{\tau_{UD}}}{\rho[1 - x(\kappa_t^2 + \kappa_r^2)]}}\right)}{\Gamma(\alpha_Z)} & x < \frac{1}{(\kappa_t^2 + \kappa_r^2)} \\ 1 & x > \frac{1}{(\kappa_t^2 + \kappa_r^2)} \end{cases} \quad (24)$$

Substituting (24) into (23), the average EC can be expressed by

$$\bar{C}_D = \frac{1}{\ln 2 \Gamma(\alpha_Z)} \int_0^{\frac{1}{(\kappa_t^2 + \kappa_r^2)}} \frac{\Gamma\left(\alpha_Z, \beta_Z \sqrt{\frac{x d_{SU}^{\tau_{SU}} d_{UD}^{\tau_{UD}}}{\rho[1 - x(\kappa_t^2 + \kappa_r^2)]}}\right)}{1 + x} dx. \quad (25)$$

It is difficult to obtain the closed-form expression of the average EC. Therefore, we apply the Gaussian Chebyshev [45,46] to approximate the average EC. And the approximate average EC can be obtained as

$$\bar{C}_D \approx \sum_{i=0}^I \frac{\pi \sqrt{1 - \vartheta_i^2} (\kappa_t^2 + \kappa_r^2)}{I \ln 2 (2(\kappa_t^2 + \kappa_r^2) - (1 + \vartheta_i))} \times \frac{\Gamma\left(\alpha_Z, \beta_Z \sqrt{\frac{(1 + \vartheta_i) d_{SU}^{\tau_{SU}} d_{UD}^{\tau_{UD}}}{\rho(\kappa_t^2 + \kappa_r^2)[1 - \vartheta_i]}}\right)}{\Gamma(\alpha_Z) (\kappa_t^2 + \kappa_r^2)}. \quad (26)$$

where $\vartheta_i = \cos\left(\frac{2i-1}{2I}\pi\right)$.

4. Numerical results and Discussion

This section presents numerical findings from the previously developed expressions to validate the preceding study. Monte Carlo simulations are used to validate the outcomes as [47–50]. In the absence of alternative specifications, the parameters are established

as follows: $r_U = 10$ [m], $\varphi_U = \pi/8$, $(x_S, y_S, 0) = (10, 5, 0)$ [m], $(x_D, y_D, 0) = (-10, 5, 0)$ [m], $\alpha_1 = \kappa_0$, $\alpha_2 = 2/\pi \ln(\kappa_{\pi/2}/\kappa_0)$, $\kappa_0 = 5$ dB, $\kappa_{\pi/2} = 15$ dB, $\alpha_3 = -1.5$, $\alpha_4 = 3.5$, $\alpha_5 = 4.88$, $\alpha_6 = 0.43$, $\kappa_t^2 = \kappa_r^2 = 0.01$, $R_{th} = 0.1$ [b/s/Hz], and $N = 8$.

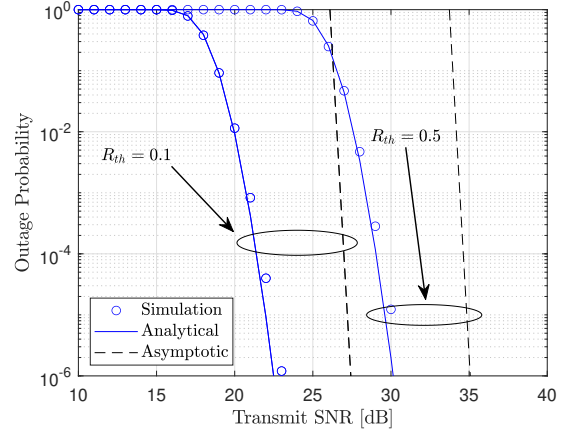


Fig. 2: Outage probability versus transmit SNR [dB] with the different of target rate R_{th} .

In Figure 2, we plot the OP versus transmit SNR in dB with different target rates R_{th} . As can be observed, the simulation, analytical, and asymptotic results are perfectly matching to verify our analysis. Furthermore, the outage performance is significantly improved when transmit SNR increases to 15 dB for $R_{th} = 0.1$ [b/s/Hz] and 25 dB for $R_{th} = 0.5$ [b/s/Hz]. In addition, when decreasing the target rate R_{th} , it leads to a smaller threshold for OP. Thus, the outage performance is also improved.

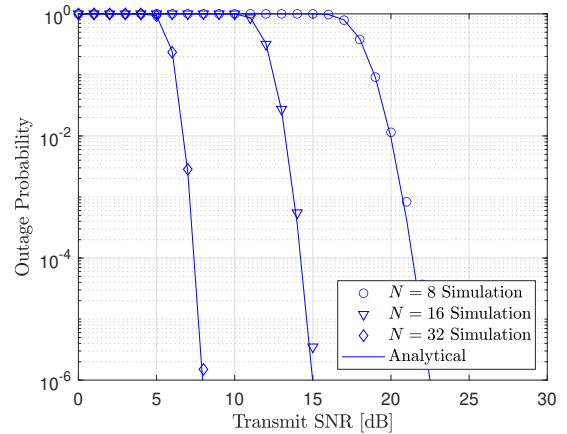


Fig. 3: Outage probability versus transmit SNR [dB] with varying the number of reflecting elements N .

Figure 3 presents the OP as a function of the transmit SNR in dB for different numbers of reflecting elements N . The simulation, analytical, and asymptotic results exhibit a near-perfect agreement, thereby confirming the accuracy of the proposed analysis. Further-

more, increasing the number of reflecting elements N enhances the outage performance, particularly at low SNR values. Specifically, to achieve an outage probability of 10^{-6} , an SNR of 22.5 dB is required when $N = 8$, whereas the required SNR decreases to 15 dB and 8 dB for $N = 16$ and $N = 32$, respectively. This result highlights the advantage of increasing N , as the system can achieve the desired performance with lower transmit power levels.

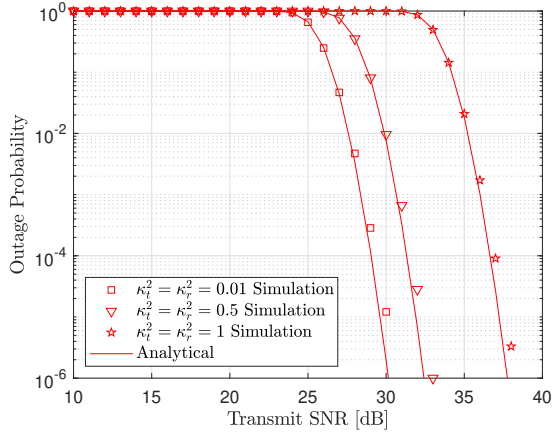


Fig. 4: Outage probability versus transmit SNR [dB] with varying the factor of hardware impairments.

Figure 4 illustrates the simulation results of OP versus SNR in dB for various hardware impairment factors κ . The results demonstrate the impact of hardware impairments on system performance. Specifically, as hardware impairments increase, a higher SNR is required to achieve the same OP. For instance, to achieve an OP of 10^{-6} , an SNR of around 30 dB is required when $\kappa = 0.01$, whereas the required SNR increases to 32 dB and 38 dB for $\kappa = 0.5$ and $\kappa = 1$, respectively. This finding underscores the detrimental effect of hardware impairments, as achieving the desired system performance necessitates higher transmit power levels.

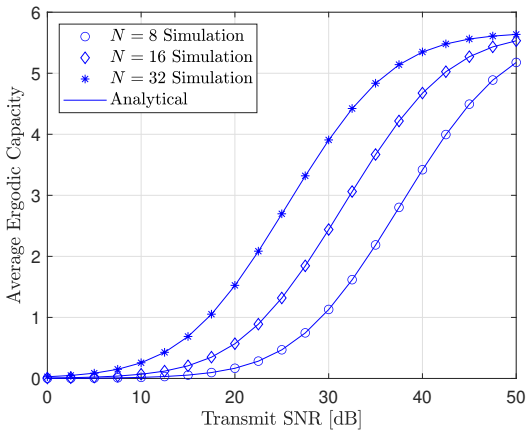


Fig. 5: Average ergodic capacity versus transmit SNR [dB] with varying the number of reflecting elements N .

Figure 5 depicts the EC versus SNR (dB) varying the number of reflecting elements N . At low SNR levels, the gaps between the curves are pronounced, indicating a substantial improvement in average capacity as N increases. However, the curves converge to a single point at the higher SNR level, suggesting that the impact of increasing the number of reflecting elements becomes marginal at high SNR levels, resulting in minimal differences in ergodic capacity.

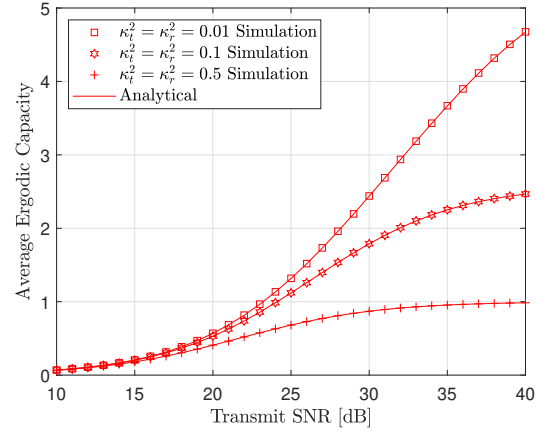


Fig. 6: Average ergodic capacity versus transmit SNR [dB] with varying the factor of hardware impairments and $N = 16$.

Figure 6 illustrates several curves of EC versus SNR (dB) for different hardware impairment factors κ , with $N = 16$. The results demonstrate the influence of hardware impairment levels on EC. Specifically, as the value of κ decreases, the gap between the curves becomes more pronounced at higher SNR levels, highlighting the increasing impact of hardware impairments on system performance as the SNR grows.

5. Conclusion

This work considered the performance of the RIS-equipped UAV communication network under the impact of hardware impairments. Furthermore, the closed-form, approximated expression of OP and average EC, and the asymptotic OP are also expressed to evaluate the performance of our proposed system. Moreover, Monte Carlo Simulation is employed to verify the analysis and show the performance of the system. The performance is significantly improved when increasing the transmit power, number of elements of UAV-RIS, and decreasing the factor of hardware impairments.

This study established a precise mathematical framework for performance assessment; yet, it presents various avenues for future research, including multi-antenna sources, energy harvesting challenges, and imperfect channels.

Acknowledgment

The authors extend their sincere gratitude to the anonymous reviewers for their insightful comments and constructive suggestions, which have significantly contributed to the improvement of this study. This work is a part of the research project CSB2024-06 funded by Saigon University.

Author Contributions

N.-T. N. performed the analytic calculations and performed the numerical simulations. H.-N. N. and M.V. B. wrote the whole paper. All authors contributed to the final version of the manuscript.

References

- [1] LE, A. -T., et al. Power Beacon and NOMA-Assisted Cooperative IoT Networks With Co-Channel Interference: Performance Analysis and Deep Learning Evaluation. *IEEE Transactions on Mobile Computing*. 2024, vol. 23, no. 6, pp. 7270-7283. DOI: 10.1109/TMC.2023.3333764.
- [2] HUNG, N., et al. Security-Reliability Analysis in CR-NOMA IoT Network Under I/Q Imbalance. *IEEE Access*. 2023, vol. 11, pp. 119045-119056. DOI: 10.1109/ACCESS.2023.3327789.
- [3] AOUEDI, O., et al. A Survey on Intelligent Internet of Things: Applications, Security, Privacy, and Future Directions. *IEEE Communications Surveys & Tutorials*. 2025, vol. 27, no. 2, pp. 1238-1292. DOI: 10.1109/COMST.2024.3430368.
- [4] ARZYKULOV, S. , G. NAURYZBAYEV, M. S. HASHMI, A. M. ELTAWIL, K. M. RABIE, and S. SEILOV. Hardware- and interference-limited cognitive IoT relaying NOMA networks with imperfect SIC over generalized non-homogeneous fading channels. *IEEE Access*. 2020, vol. 8, pp. 72942-72956. DOI: 10.1109/ACCESS.2020.2987873.
- [5] BUZZI, S., C.-L. I, T. E. KLEIN, H. V. POOR, C. YANG, and A. ZAPPONE. A survey of energy-efficient techniques for 5G networks and challenges ahead. *IEEE J. Sel. Areas Commun.* 2016, vol. 34, no. 4, pp. 697-709. DOI: 10.1109/JSAC.2016.2550338.
- [6] HUNG, T. C. , T. N. NGUYEN, V. Q. SY, A. -T. LE, B. V. MINH and M. VOZNAK. Performance Analysis of Ergodic Rate and Effective Capacity for RIS-Assisted NOMA Networks Over Nakagami-m Fading Environments. *IEEE Access*. 2024, vol. 12, pp. 181271-181281. DOI: 10.1109/ACCESS.2024.3509856.
- [7] YANG, P., L. YANG and S. WANG. Performance Analysis for RIS-Aided Wireless Systems With Imperfect CSI. *IEEE Wireless Communications Letters*. 2022, vol. 11, no. 3, pp. 588-592. DOI: 10.1109/LWC.2021.3136930.
- [8] LE, A. -T., et al. Physical layer security analysis for RIS-aided NOMA systems with non-colluding eavesdroppers. *Computer Communications*. 2024, vol. 219, pp. 194-203. DOI: 10.1016/j.comcom.2024.03.011.
- [9] DASH, S. P. , R. K. MALLIK and N. PANDEY. Performance Analysis of an Index Modulation-Based Receive Diversity RIS-Assisted Wireless Communication System. *IEEE Communications Letters*. 2022, vol. 26, no. 4, pp. 768-772. DOI: 10.1109/LCOMM.2022.3147804.
- [10] LE, A. -T. et al. Performance Analysis of RIS-Assisted Ambient Backscatter Communication Systems. *IEEE Wireless Communications Letters*. 2024, vol. 13, no. 3, pp. 791-795. DOI: 10.1109/LWC.2023.3344113.
- [11] ZHANG, B., K. YANG, K. WANG and G. ZHANG. Performance Analysis of RIS-Assisted Wireless Communications With Energy Harvesting. *IEEE Transactions on Vehicular Technology*. 2023, vol. 72, no. 1, pp. 1325-1330. DOI: 10.1109/TVT.2022.3205448.
- [12] NGUYEN, N. -L., S. -P. LE, A. -T. LE, N. D. NGUYEN, D. -T. DO and M. VOZNAK. UAV-Based Satellite-Terrestrial Systems With Hardware Impairment and Imperfect SIC: Performance Analysis of User Pairs. *IEEE Access*. 2021, vol. 9, pp. 117925-117937. DOI: 10.1109/ACCESS.2021.3107253.
- [13] ZHAN, P., K. YU and A. L. SWINDLEHURST. Wireless Relay Communications with Unmanned Aerial Vehicles: Performance and Optimization. *IEEE Transactions on Aerospace and Electronic Systems*. 2011, vol. 47, no. 3, pp. 2068-2085. DOI: 10.1109/TAES.2011.5937283.
- [14] MUHAMMAD HASHIR, S., A. MEHRABI, M. R. MILI, M. J. EMADI, D. W. K. NG and I. KRIKIDIS. Performance Trade-Off in UAV-Aided Wireless-Powered Communication Networks via Multi-Objective Optimization. *IEEE Transactions on Vehicular Technology*. 2021, vol. 70, no. 12, pp. 13430-13435. DOI: 10.1109/TVT.2021.3122077.

- [15] MINH, B. V., et al. Performance Prediction in UAV-Terrestrial Networks With Hardware Noise. *IEEE Access*. 2023, vol. 11, pp. 117562-117575. DOI: 10.1109/ACCESS.2023.3325478.
- [16] HAYAT S., E. YANMAZ, and R. MUZAF-FAR. Survey on unmanned aerial vehicle networks for civil applications: A communications viewpoint. *IEEE Commun. Surveys Tuts*. 2016, vol. 18, no. 4, pp. 2624-2661. DOI: 10.1109/COMST.2016.2560343.
- [17] GUPTA, L., R. JAIN, and G. VASZKUN. Survey of important issues in UAV communication networks. *IEEE Commun. Surveys Tuts*. 2016, vol. 18, no. 2, pp. 1123-1152. DOI: 10.1109/COMST.2015.2495297.
- [18] MOTLAGH, N. H., T. TALEB, and O. AROUK. Low-altitude unmanned aerial vehicles-based Internet of Things services: Comprehensive survey and future perspectives. *IEEE Internet Things Journal*. 2016, vol. 3, no. 6, pp. 899-922. DOI: 10.1109/JIOT.2016.2612119.
- [19] KRISHNA, C. G. L. and R. R. MURPHY. A review on cybersecurity vulnerabilities for unmanned aerial vehicles. *IN Proc. IEEE Int. Symp. Safety Security Rescue Robot (SSRR), Shanghai, China*. 2017, pp. 194-199. DOI: 10.1109/SSRR.2017.8088163.
- [20] JIANG, J. and G. HAN. Routing protocols for unmanned aerial vehicles. *IEEE Commun. Mag*. 2018, vol. 56, no. 1, pp. 58-63. DOI: 10.1109/MCOM.2017.1700326.
- [21] NGUYEN, TAN N., et al. On the dilemma of reliability or security in unmanned aerial vehicle communications assisted by energy harvesting relaying. *IEEE Journal on Selected Areas in Communications*. 2023, vol. 42, No. 1, pp. 52-67. DOI: 10.1109/JSAC.2023.3322756.
- [22] CHEN Y., and W. CHENG. Performance Analysis of RIS-equipped-UAV Based Emergency Wireless Communications. *ICC 2022 - IEEE International Conference on Communications*. 2022, pp. 255-260. DOI: 10.1109/ICC45855.2022.9839157.
- [23] PENCHALA, S., S. K. BANDARI, and V. V. MANI. Performance evaluation of RIS mounted UAV communication system with RF energy harvesting. *Telecommunication Systems*. 2025, vol. 88, no. 1. DOI: 10.1007/s11235-025-01262-6.
- [24] CHEN, Y., W. CHENG and W. ZHANG. Reconfigurable Intelligent Surface Equipped UAV in Emergency Wireless Communications: A New Fading-Shadowing Model and Performance Analysis. *IEEE Transactions on Communications*. 2024, vol. 72, no. 3, pp. 1821-1834. DOI: 10.1109/TCOMM.2023.3336223.
- [25] NGUYEN, M. -H. T., E. GARCIA-PALACIOS, T. D.-DUY, O. A. DOBRE and T. Q. DUONG. UAV-Aided Aerial Reconfigurable Intelligent Surface Communications With Massive MIMO System. *IEEE Transactions on Cognitive Communications and Networking*. 2022, vol. 8, no. 4, pp. 1828-1838. DOI: 10.1109/TCCN.2022.3187098.
- [26] LE, S-P., et al. On the Secrecy Performance of Reconfigurable Intelligent Surfaces-Assisted Satellite Networks Under Shadow-Rician Channels. *IEEE Transactions on Aerospace and Electronic Systems*. 2025, pp. 1-14. DOI: 10.1109/TAES.2025.3532227.
- [27] LE, A-T., et al. On Performance of Cooperative Satellite-AAV-secured Reconfigurable Intelligent Surface Systems with Phase Errors. *IEEE Communications Letters*. 2025, vol. 29, No. 4, pp. 799-803. DOI: 10.1109/LCOMM.2025.3543732.
- [28] LE, A-T., et al. Partial Multiplexing Power-Frequency Multiple Access for Active STAR-RIS Systems: Outage and Ergodic Perspectives. *IEEE Wireless Communications Letters*. 2024, vol. 14, No. 3, pp. 786-790. DOI: 10.1109/LWC.2024.3523387.
- [29] LE, A-T., et al. Active Reconfigurable Repeater-Assisted NOMA Networks in Internet-of-Things: Reliability, Security, and Covertness. *IEEE Internet of Things Journal*. 2024, vol. 12, No. 7, pp. 8759-8772. DOI: 10.1109/LWC.2024.3523387.
- [30] ZETTERBERG, P. Experimental investigation of TDD reciprocity-based zeroforcing transmit precoding. *EURASIP J. Adv. Signal Process*. 2011, vol. 2011, no. 1, pp. 1-10. DOI: 10.1155/2011/137541.
- [31] PHU, T-T., et al. Throughput enhancement for multi-hop decode-and-forward protocol using interference cancellation with hardware imperfection. *Alexandria Engineering Journal*. 2021, vol. 61, no. 8, pp. 5837-5849. DOI: 10.1016/j.aej.2021.11.008.
- [32] YANG L., F. MENG, J. ZHANG, M. O. HASNA and M. D. RENZO. On the Performance of RIS-Assisted Dual-Hop UAV Communication Systems. *IEEE Transactions on Vehicular Technology*. 2020, vol. 69, no. 9, pp. 10385-10390. DOI: 10.1109/TVT.2020.3004598.
- [33] YANG L., P. LI, F. MENG and S. YU. Performance Analysis of RIS-Assisted UAV Communication Systems. *IEEE Transactions on Vehicular*

- Technology. 2022, vol. 71, no. 8, pp. 9078-9082. DOI: 10.1109/TVT.2022.3175964.
- [34] AGRAWAL N., A. BANSAL, K. SINGH and C. -P. LI. Performance Evaluation of RIS-Assisted UAV-Enabled Vehicular Communication System With Multiple Non-Identical Interferers. *IEEE Transactions on Intelligent Transportation Systems*. 2022, vol. 23, no. 7, pp. 9883-9894. DOI: 10.1109/TITS.2021.3123072.
- [35] BOULOGEORGOS A. -A. A., A. ALEXIOU and M. D. RENZO. Outage Performance Analysis of RIS-Assisted UAV Wireless Systems Under Disorientation and Misalignment. *IEEE Transactions on Vehicular Technology*. 2022, vol. 71, no. 10, pp. 10712-10728. DOI: 10.1109/TVT.2022.3187050.
- [36] YANG, L., P. LI, F. MENG and S. YU. Performance analysis of RIS-assisted UAV communication systems. *IEEE Transactions on Vehicular Technology*. 2022, vol. 71, no. 8, pp. 9078-9082. DOI: 10.1109/TVT.2022.3187050.
- [37] MATOLAK, D. W., SUN R. Unmanned aircraft systems: Air-ground channel characterization for future applications. *IEEE Vehicular Technology Magazine*. 2015, vol. 10, no. 2, pp. 79-85. DOI: 10.1109/MVT.2015.2411191.
- [38] AZART, M. M., F. ROSAS, K. C. CHEN and S. POLLIN. Ultra reliable UAV communication using altitude and cooperation diversity. *IEEE Transactions on Communications*. 2017, vol. 66, no. 1, pp. 330-344. DOI: 10.1109/TCOMM.2017.2746105.
- [39] SONG Q., F. C. ZHENG, Y. ZENG and J. ZHANG. Joint beamforming and power allocation for UAV-enabled full-duplex relay. *IEEE Transactions on Vehicular Technology*. 2018, vol. 68, no. 2, pp. 1657-1671. DOI: 10.1109/TVT.2018.2889349.
- [40] T. -H. VU, et al. Intelligent Reflecting Surface-Aided Short-Packet Non-Orthogonal Multiple Access Systems. *IEEE Transactions on Vehicular Technology*. 2022, vol. 71, no. 4, pp. 4500-4505. DOI: 10.1109/TVT.2022.3146856.
- [41] BASAR, E. et al. Wireless communications through reconfigurable intelligent surfaces. *IEEE access*. 2019, vol. 7, pp. 116753-116773. DOI: 10.1109/ACCESS.2019.2935192.
- [42] DO D. T., A. T. LE, Y. LIU and A. JAMALIPOUR. User grouping and energy harvesting in UAV-NOMA system with AF/DF relaying. *IEEE Transactions on Vehicular Technology*. 2021, vol. 70, no. 11, pp. 11855-11868. DOI: 10.1109/TVT.2021.3116101.
- [43] NGUYEN, T-N., et al. Two-Way Half Duplex Decode and Forward Relaying Network with Hardware Impairment over Rician Fading Channel: System Performance Analysis. *Elektronika Ir Elektrotechnika*. 2018, vol. 24, no. 2, pp.74-78. DOI: 10.5755/j01.eie.24.2.20639.
- [44] NGUYEN, T-N., et al. Adaptive Relaying Protocol for Decode and Forward Full-Duplex System over Rician Fading Channel: System Performance Analysis. *China Communications*. 2019, vol. 16, no. 3, pp. 92-102. DOI: 10.12676/j.cc.2019.03.009.
- [45] VO, D. -T., T. N. NGUYEN, A. -T. LE, V. -D. PHAN and M. VOZNAK. Holographic Reconfigurable Intelligent Surface-Aided Downlink NOMA IoT Networks in Short-Packet Communication. *IEEE Access*. 2024, vol. 12, pp. 65266-65277. DOI: 10.1109/ACCESS.2024.3397306.
- [46] LE, A. T., T. -H. VU, T. TRUNG DUY, L. -T. TU and M. VOZNAK. Analysis of PHY-Layer Security and Covert Communication in Hybrid Power-Frequency Multiple Access Systems. *IEEE Wireless Communications Letters*. 2025, vol. 14, no. 2, pp. 519-523. DOI: 10.1109/LWC.2024.3514655.
- [47] NGUYEN, TAN N., et al. Performance enhancement for energy harvesting based two-way relay protocols in wireless ad-hoc networks with partial and full relay selection methods. *Ad-hoc networks*. 2019, vol.84, pp. 178-187. DOI: 10.1016/j.adhoc.2018.10.005.
- [48] NGUYEN, TAN N., et al. Energy harvesting over Rician fading channel: a performance analysis for half-duplex bidirectional sensor networks under hardware impairments. *Sensors*. 2018, vol. 18, no. 6, pp. 1-22. DOI: 10.3390/s18061781.
- [49] V. -D. PHAN, et al. Performance of Cooperative Communication System With Multiple Reconfigurable Intelligent Surfaces Over Nakagami-m Fading Channels. *IEEE Access*. 2022, vol. 10, pp. 9806-9816. DOI: 10.1109/ACCESS.2022.3144364.
- [50] T. -N. NGUYEN, et al. Performance Evaluation of User Selection Protocols in Random Networks with Energy Harvesting and Hardware Impairments. *Advances in Electrical and Electronic Engineering journal*. 2016, vol. 14, no. 4, pp. 372-377. DOI: 10.15598/aeec.v14i4.1783.
- [51] GRADSHTEYN I. S. and I. M. RYZHIK, *Table of Integrals, Series and Products*, 7th ed. New York, NY, USA: Academic, 2007. DOI: 10.1016/C2010-0-64839-5.